engineering proceedings

MDPI

Proceeding Paper

Ancient Projectile Identification Through Inverse Analysis: Case Studies from Pompeii †

Simone Palladino, Renato Zona and Vincenzo Minutolo *

Department of Engineering, University of Campania "L. Vanvitelli", 81031 Aversa, Italy; simone.palladino@unicampania.it (S.P.); renato.zona@unicampania.it (R.Z.)

* Correspondence: vincenzo.minutolo@unicampania.it

† Presented at the Conference "Discovering Pompeii: From Effects to Causes—From Surveying to the Reconstructions of Ballistae and Scorpiones", Aversa, Italy, 27 February 2025.

Abstract: A straightforward method for determining the causes of impact relics left by ancient projectiles on the city walls of Pompeii is proposed based on principles of plasticity and fracture mechanics. The inverse analysis begins with the measured craters caused by spherical projectiles or darts launched by the Roman army during the siege of 89 B.C. A Mathematica© notebook is presented, enabling the calculation of projectile impact velocity from the known dimensions of the projectiles and the mechanical properties of the wall material.

Keywords: inverse analysis; ancient ballista; fracture release rate; plastic dissipation

1. Introduction

The work is aimed at evaluating the characteristics of ancient war machines such as the ballista in Roman times. The study is focused on the relic of the impact of projectiles on some of Pompei's walls that were the object of siege during Silla's campaign in 89 B.C. [1,2]. The geometry of impact craters offers essential clues about the dynamics of the impacting projectiles. Inverse analysis is implemented to relate the estimated energy dissipation for producing impact craters and the momentum of the projectiles. In the outer walls of the City of Pompei, two principal signs of impact can be recognized: the first, a large crater of about 140 mm, seems to be created by the impact of a spherical projectile from a fixed ballista; the second, a small conical hole, with the diameter of about few centimeters, $\phi_d = 30$ mm, seems to be caused by an ancient automatic portable ballista able to shot light darts whose mass was $m_d = 150$ g called *polybolos* [3–8]. The main parameters one should define to carry out the analyses are the mechanical properties of the wall of the City. The material constituting the structure is grey tuff, of the Neapolitan area, namely Nocera's tuff. Mechanical properties of the material suggest addressing the derivation of the breakage parameters of the material from analogous studies made on the resistance and the collapse of soils and rocks [9–11]. Work [12] employs the Mohr–Coulomb failure criterion and limit analysis via a paraboloidal collapse surface to derive closed-form solutions for masonry structure collapse and energy dissipation. Similarly, refs. [13,14] emphasize how porosity and heterogeneity affect collapse loads and apply a limit analysis procedure for evaluating the collapse load of masonry domes. Recent studies have also focused on the fracture behavior of volcanic rocks as natural materials and as reinforcing phases in composites. Fracture toughness, often quantified via the critical energy release rate (G_f) or the stress intensity factor (Sif), serves as a fundamental indicator of a material's resistance to crack propagation under linear elastic fracture mechanics. The propagation and coalescence of

check for updates

Published: 6 June 2025

Citation: Palladino, S.; Zona, R.; Minutolo, V. Ancient Projectile Identification Through Inverse Analysis: Case Studies from Pompeii. *Eng. Proc.* **2025**, *96*, 8. https://doi.org/10.3390/engproc2025096008

Copyright: © 2025 by the authors. Licensee MDPI, Basel, Switzerland. This article is an open access article distributed under the terms and conditions of the Creative Commons Attribution (CC BY) license (https://creativecommons.org/licenses/by/4.0/).

fractures are studied in several papers [15–19] where the propagation and the load-bearing capacities of structures made of heterogeneous and no tension materials are presented.

By analyzing post-impact deformation and fracture patterns, in the paper, the velocity of projectiles quantifying momentum transfer and impact energy absorption is analyzed. Special emphasis is placed on evaluating energy dissipation via localized cracking and plastic energy accumulation at fracture sites. Ballista spherical projectiles and dart projectiles of portable ballista effects are simulated using different strategies that perform the calculation based on a static approach that results faster and more robust with respect to transient dynamics numerical analysis. Through the described methods, we calculate the projectile velocity and the energy dissipation produced by shooting from the measured impact holes directly.

The paper presents the results of a finite element program under static loading, simulating the applied force due to the impact on a point of the wall. The material of the wall is grey tuff, and the projectile is described with the equivalent one-point force. The intensity of the force at the collapse of the application point neighborhood is evaluated, and the permanent strain amount is used to calculate dissipated energy corresponding to the transformation of the kinetic energy of the projectile. In a second approach, the fracture energy required for breaking the material volume of the wall at the impact target, whose dimensions were detected in [3–5], is related to kinetic energy as well to obtain projectile impact velocity.

Finally, the elastic energy accumulated during the loading process in the impact is compared with the fracture release energy to verify the balance in the framework of the linear fracture mechanics theory.

Conclusions and discussion highlight the feasibility of the strategies that are able to evaluate compatible velocity and the momentum of the projectiles of the ancient Roman war machines during I century B.C.

2. Materials and Methods

The inverse analysis of the effects of ancient projectiles on the wall structures of cities is described considering direct energy evaluation. Numerical calculations are the main strategy nowadays used due to the great affordably of FEM modeling. However, a direct calculation based on simple models that use mechanics and descriptions of the phenomena can give valuable indications on the order of magnitude and straightforward results to make an inverse analysis.

The impact of the projectile on the wall dissipates energy in several manners; the most is ascribed to the energy to produce irreversible deformation. To evaluate the dissipated energy, two strategies are implemented in the work.

Ductile Plastic Dissipation by FEM

At first, we implemented static calculation using an elastoplastic model of ductile dissipation. The wall structure was loaded with one nodal force up to the structure collapse that involved locally an imitated number of elements, as is to be expected in a point load problem. The irreversible strain at the incoming collapse measures the stress–strain dissipation, namely the deviatoric stress acting on the elements where the plastic strain accumulates so works that cannot be recovered. The resulting plastic dissipation is equated to the kinetic energy of the projectile resulting in its velocity.

The dimensions of the wall were considered from the measures reported in [4]. A preliminary study was conducted to recognize the mesh size and the wall dimensions so that boundary effects could be neglected. The geometric properties of the wall and the corresponding mechanical parameters are shown in Table 1.

Table 1. Mechanical properties of the target wall.

Young Modulus (E)	2914 MPa
Poisson Coefficient (ν)	0.29
Yield Stress (σ_Y)	4.47 MPa

At the incoming collapse, the plastic dissipation can be evaluated through the permanent strain and corresponding yield stress.

$$D^p = \int_B \int_{t_0}^{t_c} \sigma_0 \dot{\varepsilon}^p dt dV = \int_B \sigma_0 \varepsilon^p dV \quad (1)$$

Equation (1) is obtained assuming the normality flaw rule and perfect plasticity; hence, the deviatoric stress is constant in time, and permanent strain reduces to accumulated permanent strain that has no components along with the hydrostatic stress line.

In the FEM result, the permanent strain deviatoric norm was multiplied for the deviatoric stress yielding and integrated over the element volume, resulting in

$$D^p = \sum_{e=1}^{pe} \sigma_{de} \varepsilon_{de}^p V_e \quad (2)$$

By considering the complete transformation of the kinetic energy of the dart into plastic dissipation, one can evaluate

$$\frac{1}{2} m_d v_d^2 = D^p \quad (3)$$

that results in

$$v_p = \sqrt{\frac{2D^p}{m_d}} \quad (4)$$

The second approach is based on the fracture energy capable of breaking the projectile target volume into pieces. The involved volume is derived from the dimensions of the measured holes detected in the observation of ancient relics.

The inverse analysis allowed us to recognize the velocities of the projectile from the probable dimensions of fragments.

The procedure is based on some hypotheses, namely that the fragments have a polyhedral shape; in particular, an icosahedral shape was assumed, and the surface area of the polyhedron was calculated considering the presence of perturbation of the side plane. The perturbation was modeled by using pyramidal protrusions. It is known that the pyramid side surface is $\beta = \sqrt{5} = 2.24$ times the base area. Hence, the amplification coefficient β was introduced, yielding to the evaluation of the effective surface of the crack opening to break the target into pieces

$$S_f = \beta \cdot 5\sqrt{3}\phi^2 \quad (5)$$

where ϕ is the dimension of the face of the icosahedron. The relationship that links the diameter of the sphere that is circumscribed to the icosahedron D_s is

$$f = \sqrt{0.5 - \frac{\sqrt{5}}{10} D_s} \quad (6)$$

In Equation (5), the surface refers to a single fragment, and the fragment volume is given by

$$V_f = \frac{5}{12}\left(\sqrt{5} + 3\right)\phi^3 \quad (7)$$

Equation (7) allows calculating the number of fragments in the volume of the detected hole.

$$V_H = \pi d_H^2 \left(\frac{D}{2} - \frac{d_H}{3} \right) \tag{8}$$

$$n_f = \frac{V_H}{V_f} \tag{9}$$

Finally, the dissipated energy due to crack openings is

$$E_f = n_f G_f \frac{S_f}{2} \sqrt{5} \tag{10}$$

where the denominator 2, under the surface term S_f, accounts for the presence of two surfaces at any crack openings.

To obtain the sought impact velocity, the energy (10) is equated to the kinetic energy of the projectile

$$k = \frac{1}{2} m_p v_p^2 \tag{11}$$

so that

$$v_p = \sqrt{\sqrt{5} \frac{n_f G_f S_f}{m_p}} \tag{12}$$

3. Results

The procedures described in the previous section were applied to the structure of Pompei's wall reported in [4]. The materials' properties and the geometry were derived from the literature, and the two approaches that can be summarized as ductile and fragile are reported hereafter.

3.1. FEM Ductile Plastic Analysis

The FEM model simulates the target wall whose properties are reported in Table 1.

The FEM analysis was carried out to obtain the final configuration of the local collapse due to the impact of a dart with a mass of 0.150 kg using a step-by-step collapse calculation. The collapse load was calculated as follows:

$$F_c = 20 \text{ kN} \tag{13}$$

The geometry, mesh, and von Mises stress are depicted in Figure 1, where the stress concentration at the incoming collapse around the impact area is highlighted.

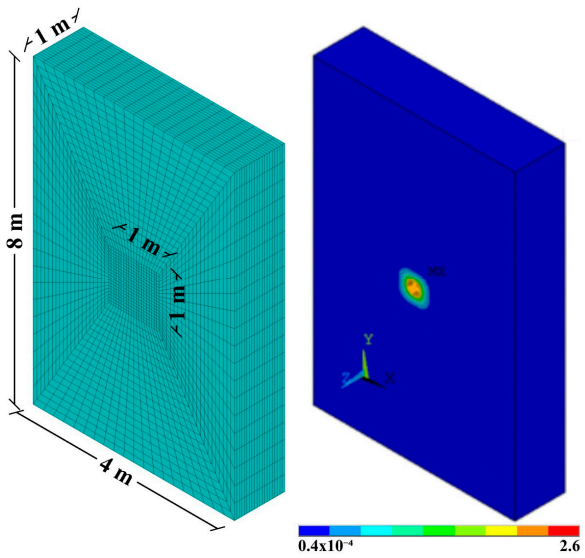


Figure 1. Finite element mesh refinement prescribed in the impact area (**left**). The contour plot of the von Mises stress, corresponding to the incoming collapse around the impact area (**right**).

The FEM calculation furnished plastic dissipation D^p at the incoming collapse given by

$$D^p = 15.91 \text{ kJ} \tag{14}$$

that allows calculating the dart velocity from Equation (4) as

$$v_D = \sqrt{\frac{2 \cdot 15.91}{0.150}} = 14.56 \text{ m s}^{-1} \tag{15}$$

3.2. Fragile Procedure via Fracture Energy Release

The fracture energy release of the material constituent of the wall, G_f, is obtained from literature reports about volcanic materials [13]; it is calculated from the critical Stress Intensity Factor $KI_c = 1.5$ MPa $\sqrt{}$m:

$$G_f = \frac{KI_c^2}{E} = 0.81 \text{ kJ m}^{-2} \tag{16}$$

3.3. The Ballista Spherical Projectile

As a first application of the method, the case of a projectile of a ballista constituted by a basalt sphere was considered.

Ballista projectile impact over the wall produced a hemispherical hole whose surface is characterized by several fragment tracks. The average dimension of the fragments was detected and reported in the reconstruction made in [5].

The geometric characteristics of the impact track are reported in Table 2.

Table 2. The geometry of the projectile and relics on the wall.

Diameter D	Density ρ	Hole Depth d_H	Hole Volume V_H	Mass m_p
140 mm	2.800 kg m^3	120 mm	$1.149 \cdot 10^{-2}$ m^3	3.22 kg

The fragment radius is considered by observation of the dimensions of tracks on the 3D reconstruction of the shots imaging reported in [4]. In Figure 2, a sample of the 3D reconstruction is depicted. The yellow drawings in the picture highlight the shape and the dimensions of probable fragments of the material destroyed by the shooting. The dimensions of the pieces can be evaluated considering that the projectile marks on the wall have the diameter reported in Table 2 D = 140 mm. Although the marks have been smoothed by aging, the remaining signs allow recognizing an average dimension between 20 mm and 35 mm.

Relationship (12) has been applied to different fragments' dimensions in the range 0.1 mm $\leq D_s \leq$ 40 mm, yielding to the diagram reported in Figure 3.

The diagrams show that for fragment dimensions of about 20 mm $< D_s <$ 30 mm, which are the most probable to fit the measured cavity in the wall, the average projectile speed is about 15.19 ms^{-1} $< v_s <$ 12.40 ms^{-1} that corresponds to energy

$$464.0 \text{ J} < E < 309.3 \text{ J} \tag{17}$$

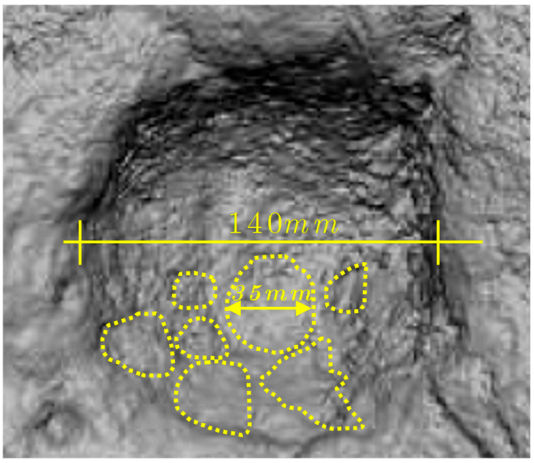


Figure 2. Three-dimensional representation of the shooting mark. Yellow indicates the traces and dimensions.

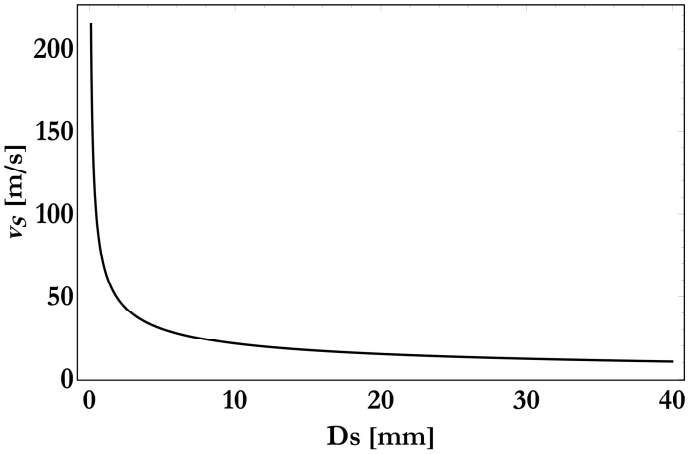


Figure 3. Spherical projectile effect: velocity versus the diameter of fragments.

3.4. Darts from Portable Ballista or Polybolos

The analysis of the effect of darts follows the same approach used for the spherical projectiles but with the modification required by the shape of the projectile tip that is pyramidal. The geometry of the dart is reported in Table 3.

Table 3. Geometry of the darts and their relics on the wall.

Base B	Height H	Density ρ	Hole Dept d_H	Hole Volume V_H	Mass m_d
30 mm	40 mm	7.800 kg m^3	40 mm	$8.559 \cdot 10^{-6}$ m^3	0.15 kg

Using the same equation as for the spherical projectile, except for the hole shape and volume, the following representation of the velocity–fragment diagram is obtained (see Figure 4).

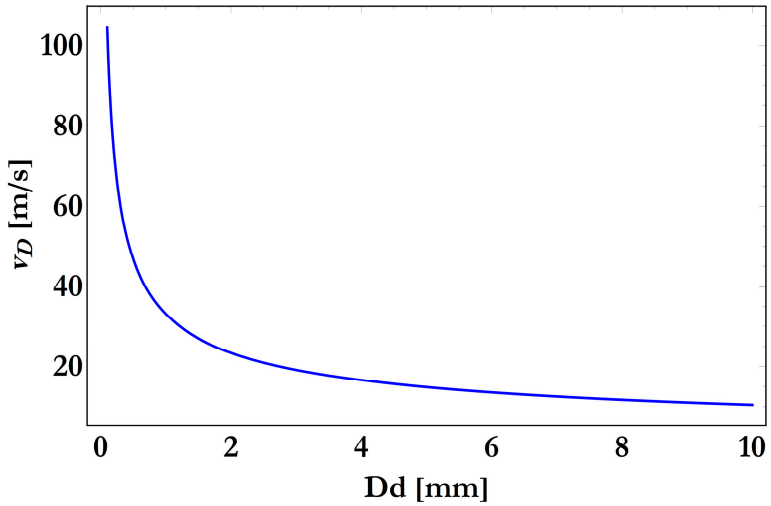


Figure 4. Dart effect: velocity of projectile versus the diameter of prevised fragments.

The results summarize the dart effect as follows:

$$4\ \text{mm} < D_d < 6\ \text{mm} \rightarrow 16.54\ \text{ms}^{-1} < v_D < 13.50\ \text{ms}^{-1} \quad (18)$$

that corresponds to the energy

$$20.52\ \text{J} < E < 13.67\ \text{J} \quad (19)$$

A final consideration about the fracture energy release method can be made considering that the energy release for the fracture to develop can be associated with strain energy recovery due to the relaxation of the stress state at the impact. The idea follows from the Griffith energy release approach to fracture. We can assume that, on impact, the projectile loaded the structure by a force consequence of the deceleration. The effect is a deformation of the wall that produces elastic energy accumulation in the structure. If the accumulated elastic energy is released through fracture openings, the dissipation equates with the elastic energy. Such an approach is not suitable for identification purposes since we have no information on the velocity and energy the projectile had at the impact stage. However, let us consider the force intensity equal to the collapse calculated by plastic collapse analysis. We can evaluate the strain energy at the incoming collapse, prior to plastic strain occurring, and consider the dissipated energy due to the fracture of the target as the energy release due to crack openings.

4. Discussion and Conclusions

The presented research study describes the inverse analysis of projectiles from the effects measured on the ancient Roman wall of the City of Pompei. The city walls, submerged by the Vesuvius' eruption in 79 AD, have been preserved, and the tracks of ballista shots of the Silla's army in 86 B.C. The study of the tracks is carried out considering two types of dissipative mechanisms, one due to ductile plastic dissipation through permanent deformation yielding to target destruction, and the other T through considering the fracture energy release for the target fragments to separate and cause the target hole we found in the city fortification.

The proposed models are compared with the numerical calculation performed using the commercial FEM program Ansys ©, where the direct step-by-step analysis is implemented till the structural collapse. The collapse obtained through finite elements plastic analysis offers the limit load corresponding to the rupture of the target in the wall. It has to be stressed that the obtained results, even if corresponding to direct calculation in static mode, highlight that the plastic deformation is localized at the impact point and does not

involve a large distance. Consequently, the dissipated strain energy at the collapse is bound and can be easily calculated. The only drawback of such a calculation remains in the fact that no upper bound of the ductility of the structure is considered. A more detailed dynamic step-by-step analysis that considers the plastic strain evolution and impact dissipation together with the softening behavior of the crushing mechanism of fragile materials that employ a large amount of machine time and memory describes the mechanism with more detail. However, the approach proposed here offers acceptable results, as it can be seen by comparison with work [3].

The simplified analysis represented in Equations (4) or (12) offers acceptable results with respect to both FEM calculation and [3]. The simplified procedures based on the fracture energy release are implemented through a Mathematica © notebook reported in Appendix A, where the calculations are explicated for the case of the ballista that shoots large spherical projectiles and *polybalos* [4] that represent an automatic darts shooter that is able to throw many little arrows having a mass of 150 g.

The results compared with the finite element model and with the literature outfit show that the simplified approach, although very little time-consuming and requiring minimal memory allocation, it is able to offer good results and allows analyzing, with minimal effort, the effect of projectiles on the wall staring on the measure of the target destroyed volume and mechanical properties, namely the elastic parameters, plastic stress limit, and the fracture toughness obtained using the material stress intensity factor.

Author Contributions: Conceptualization, V.M., S.P. and R.Z.; methodology, V.M., S.P. and R.Z.; software, V.M.; validation, V.M., S.P. and R.Z.; formal analysis, V.M., S.P. and R.Z.; investigation, V.M., S.P. and R.Z.; resources, V.M., S.P. and R.Z.; data curation, V.M., S.P. and R.Z.; writing—original draft preparation, V.M., S.P. and R.Z.; writing—review and editing, V.M., S.P. and R.Z.; visualization, V.M., S.P. and R.Z.; supervision, V.M.; project administration, V.M.; funding acquisition, V.M. All authors have read and agreed to the published version of the manuscript.

Funding: This research was supported by the project "SCORPiò-NIDI", CUP B53D2302210 0006, funded by the Italian Ministry of Research under the PRIN (DD n.104/2022) funding initiative.

Institutional Review Board Statement: Not applicable.

Informed Consent Statement: Not applicable.

Data Availability Statement: Research data are available upon request.

Acknowledgments: The author thanks Gabriel Zuchtriegel, Director of the Archaeological Area of Pompeii, Giuseppe Scarpati, Head of the Study and Research Area, and Valeria Amoretti. The research activities are part of the MUR—PRIN 2022 project "SCORPiò-NIDI".

Conflicts of Interest: The authors declare no conflicts of interest. The funders had no role in the design of the study; in the collection, analyses, or interpretation of data; in the writing of the manuscript; or in the decision to publish the results.

Appendix A

In the appendix, a notebook for Mathematica © Wolfram Research Inc. calculates the velocity of the projectile from the hole track dimensions using fracture energy release.

The notebook consists of two modules calculating the velocity of the projectile in the case of the spherical projectile from a ballista and the pyramidal projectile from a *polybolos*.

```
Mathematica (C) notebook for calculating projectile momentum

(* Initialization of units*)

mm = 0.001 m;
J = New m;
New = kg m / s^2;
M = 1000000;
Tough = 0.00081 M J / m^2;

(* Case of the sphere projectile *)

vP[df_] := Module[{DSphere = 140 mm,
    HoleDept = 120 mm, dFrag = df mm},
   BallVol = 4 / 3 Pi (DSphere / 2) ^3;
   HoleVol = Pi HoleDept^2 (DSphere / 2 - HoleDept / 3);
   BallMass = 2800. BallVol kg / m^3;
   aico = Sqrt[0.5 - Sqrt[5.] / 10] dFrag;
  (*FragVol=4/3 Pi (dFrag/2)^3; sphere*)
   FragVol = 5 / 12 (3 + Sqrt[5.]) aico^3 ; (*icosahedron*)
   nfrag = HoleVol / FragVol;
   (*FragSurf=4 Pi (dFrag/2)^2; sphere*)
  FragSurf = 5 Sqrt[3.] aico^2;
  FractSurf = nfrag * FragSurf Sqrt[5.] / 2;
  FractEnergys = Tough FractSurf;
  ballveloc = v /. NSolve[1 / 2 BallMass v^2 == FractEnergys, v][[2]];
  BallSpeed = PowerExpand[ballveloc /. New → kg m / s^2];
  BallSpeed /. {m → 0.001 km, s → 1 / 3600 hr}]

(* Case of the darts*)

vd[df_] := Module[{B = 30. mm,
    H = 40. mm,
    h = 0.0000001 mm,
    dFrag = df mm},
   b = B / (H + h) * h;
   HoleVol = B^2 * H / 3 - b^2 h / 3;
   DartMass = 0.15 kg;
   aico = Sqrt[0.5 - Sqrt[5.] / 10] dFrag;
   (*FragVol=4/3 Pi (dFrag/2)^3; sphere*)
   FragVol = 5 / 12 (3 + Sqrt[5.]) aico^3 ; (*icosahedron*)
   nfrag = HoleVol / FragVol;
  (*FragSurf=4 Pi (dFrag/2)^2;*)
   FragSurf = 5 Sqrt[3.] aico^2;
  FractSurf = nfrag * FragSurf Sqrt[5.] / 2;
  FractEnergyd = Tough FractSurf // Simplify;
  vdart = v /. NSolve[1 / 2 DartMass v^2 == FractEnergyd, v][[2]];
  vdart /. New → kg m / s^2;
  DartSpeed = PowerExpand[vdart /. New → kg m / s^2];
  DartSpeed /. {m → 0.001 km, s → 1 / 3600 hr}]
```

References

1. Maiuri, A. Studi e richerche sulla fortificazione di Pompeii. *Monum. Antichi Pubblicati Per Cura Della Reale Accademia dei Lincei* **1929**, *33*, 113–290.
2. Russo, F.; Russo, F. *89 a.C.: Assedio a Pompei: La dinamica e le tecnologie belliche della conquista sillana di Pompei*; Flavius Edizioni: Rome, Italy, 2005.
3. Thakkar, M.M.; Ardeshiri, A.; Guagliano, M. Structural Integrity Assessment of Pompeii's City Wall under Roman Artillery Fire: A Finite Element Approach. In *Discovering Pompeii: From Effects to Causes. From Surveying to the Reconstructions of Ballistae and Scorpiones*; (under process of publication); Realcasa dell'Annunziata, Department of Engineering, Vanvitelli University: Naples, Italy, 2025.
4. Rossi, A.; Gonizzi Barsanti, S.; Bertacchi, S. Use of *Polybolos* on the City Walls of Ancient Pompeii: Assessment on the Anthropic Cavities. *Nexus Netw. J.* **2025**, *27*, 243–272. [CrossRef]
5. Rossi, A. The Survey of the Ballistic Imprints for a Renewed Image of Unearthed Pompeii. *Nexus Netw. J.* **2024**, *26*, 307–324. [CrossRef]
6. Bertacchi, S.; Gonizzi Barsanti, S.; Rossi, A. Geometry of Wall Degradation: Measuring and Visualising Impact Craters in the Northern Walls of Pompeii. *SCIRES-IT-Sci. Res. Inf. Technol.* **2024**, *14*, 111–128. [CrossRef]
7. Rossi, A.; Bertacchi, S.; Formicola, C.; Gonizzi Barsanti, S. Piccole indentazioni antropiche rinvenute nella riesumata cinta urbica di Cornelia Veneria Pompeii. *Disegnare IDEE Immagin.* **2025**, *69*, 54–67.

8. Rossi, A.; Gonizzi Barsanti, S.; Bertacchi, S. Natural or anthropic? Measurement and visualisation of wall cavities in city walls. In *Transitions, Proceedings of the 45th International Conference of Representation Disciplines Teachers*; Franco Angeli: Milano, Itlay, 2024; pp. 1957–1978, Measure/Out of Measure. [CrossRef]
9. Balme, M.R.; Rocchi, V.; Jones, C.; Sammonds, P.R.; Meredith, P.G.; Boon, S. Fracture toughness measurements on igneous rocks using a high-pressure, high-temperature rock fracture mechanics cell. *J. Volcanol. Geotherm. Res.* **2004**, *132*, 159–172. [CrossRef]
10. Cattania, C.; Rivalta, E.; Hainzl, S.; Passarelli, L.; Aoki, Y. A nonplanar slow rupture episode during the 2000 Miyakejima dike intrusion. *J. Geophys. Res. Solid Earth* **2017**, *122*, 2054–2068. [CrossRef]
11. Liu, K.; Zhao, J. Progressive damage behaviours of triaxially confined rocks under multiple dynamic loads. *Rock Mech. Rock Eng.* **2021**, *54*, 573–590. [CrossRef]
12. Minutolo, V.; Gesualdo, A.; Nunziante, L. Local Collapse in Soft Rock Bank Cavities. *J. Geotech. Geoenvironmental Eng.* **2001**, *127*, 1037–1042. [CrossRef]
13. Heap, M.J.; Violay, M.E. The mechanical behaviour and failure modes of volcanic rocks: A review. *Bull. Volcanol.* **2021**, *83*, 33. [CrossRef]
14. Zona, R.; Ferla, P.; Minutolo, V. Limit analysis of conical and parabolic domes based on semi-analytical solution. *J. Build. Eng.* **2021**, *44*, 103271. [CrossRef]
15. Zona, R.; Minutolo, V. A dislocation-based finite element method for plastic collapse assessment in solid mechanics. *Arch. Appl. Mech.* **2024**, *94*, 1531–1552. [CrossRef]
16. Pei, G.; Xiao, D.; Zhang, M.; Jiang, J.; Xie, J.; Li, X.; Guo, J. Study on the Dynamic Fracture Properties of Defective Basalt Fiber Concrete Materials Under a Freeze–Thaw Environment. *Materials* **2024**, *17*, 6275. [CrossRef] [PubMed]
17. Palladino, S.; Esposito, L.; Ferla, P.; Zona, R.; Minutolo, V. Functionally Graded Plate Fracture Analysis Using the Field Boundary Element Method. *Appl. Sci.* **2021**, *11*, 88465. [CrossRef]
18. Esposito, L.; Palladino, S.; Minutolo, V. An effective free-meshing and linear step-wise procedure to predict crack initiation and propagation. *Theor. Appl. Fract. Mech.* **2023**, *130*, 104240. [CrossRef]
19. Palladino, S.; Minutolo, V.; Esposito, L. Hybrid semi-analytical calculation of the stress intensity factor for heterogeneous and functionally graded plates. *Eng. Fract. Mech.* **2022**, *274*, 108763. [CrossRef]

Disclaimer/Publisher's Note: The statements, opinions and data contained in all publications are solely those of the individual author(s) and contributor(s) and not of MDPI and/or the editor(s). MDPI and/or the editor(s) disclaim responsibility for any injury to people or property resulting from any ideas, methods, instructions or products referred to in the content.